Available online at www.sciencedirect.com
ScienceDirect
Solid State Ionics 179 (2008) 299–304
SOLID STATE IONICS
www.elsevier.com/locate/ssi

Template synthesized high conducting silver chloride nanoplates

J.P. Tiwari *, Chepuri R.K. Rao

Functional Materials Division (FMD), Central Electrochemical Research Institute (CECRI), Karaikudi-630006, Tamilnadu, India

Received 6 November 2007; received in revised form 20 November 2007; accepted 30 January 2008

Abstract

Silver chloride was synthesized using a water-soluble polyelectrolyte as a capping agent. X-ray diffraction (XRD), scanning electron microscopy (SEM), atomic force microscopy (AFM) and differential scanning calorimetry (DSC) were employed to characterize morphology, structure and phase transition of as-prepared silver chloride. XRD, SEM and AFM confirms the formation of nanoplates of AgCl with a polygonal edge of diameter ~250–300 nm. These nanoplates are found to be thermally stable up to its melting temperature (~455 °C) with smaller value of melting enthalpy and higher room temperature conductivity values compared to pristine silver chloride ($\sigma_{\text{Nanoplate}}/\sigma_{\text{Pristine}} \approx 10^4$).

Keywords: Nanoplates; Ionic conductivity; Silver chloride; Template; Nanoionics

1. Introduction

Nanomaterials are important class of materials due to their novel electrical, optical, magnetic and mechanical [1–13] properties for various applications such as for single electron transistors [4–5], nanoelectronics [6], lasers [7], photoelectrons, and sensors [8–13] and nanoionics [14–21].

The synthesis of nanomaterials using the concept of capping agents [22–23] is recently adapted in the field of solid-state ionics for the synthesis of shape-controlled Ag^+ [16–18] ion based conductors. These newly synthesized nanomaterials are found to have very interesting properties such as mesoscopic superionic conductivity at room temperature [16] and typical phase transitions [16–17]. However, only a few systems based on Ag^+ [16–18] ion have been investigated. Clearly, more such investigations for silver ion conductors are highly desirable to establish their general character and potential for device applications [16,21].

Silver chloride is an important dilute point defect type silver ion (Ag^+) conductor [24–30]. To the best of our knowledge, there is no report on the synthesis of shape-controlled silver chloride. Here we report the shape-controlled synthesis and characterization of AgCl by using a surfactant poly (diallyldimethylammonium chloride) (PDADMAC).

2. Experimental section

The 10 ml of polymer poly (diallyldimethylammonium chloride) (PDADMAC, 35 wt.% in water, Sigma-Aldrich) was added to 50 ml of ethanol and 50 ml of distilled water under vigorous stirring at room temperature. Then 1.7 g of $AgNO_3$ (Central Drug House, India, CDH Analytical Reagent) in a mixed solvent of 40 ml ethanol and 40 ml of water were added. After 60 min of stirring, the mixture was left for rest for a week at room temperature and the precipitates were collected through centrifuging the solution. The precipates were washed carefully with water and dried at 100 °C for 2 h. A Hitachi (S-3000H) scanning electron microscope (SEM) and an atomic force microscope (AFM, Molecular Imaging, USA, having gold-coated SiN_3 cantilevers) were used to investigate the morphology of the precipitates. The X-ray diffraction (XRD) pattern was obtained using an X'Pert PRO PANalytical instrument with Cu K_α radiation. Differential scanning calorimetry (DSC) was carried out on a TA instruments (Model: SDT Q600) under nitrogen atmosphere in the temperature range of 25 °C < T < 720 °C at a heating rate of 10 °C/min using alumina as a standard. The electrical measurements on the sample

* Corresponding author. Tel.: +91 4565 227550 559x355; fax: +91 4565 227713.
E-mail address: jai_ti2002@yahoo.com (J.P. Tiwari).

0167-2738/$ - see front matter © 2008 Elsevier B.V. All rights reserved.
doi:10.1016/j.ssi.2008.01.097

(at room temperature) are performed on a uniaxially pressed (using high chromium–high carbon steel die at a pressure of ~4 tons/cm^2) pellet (area ~54.11 mm^2 and of thickness ~4.15 mm) by two probe measurement using SI 1260 (Schlumberger) impedance analyzer with 1296 (solartron) dielectric interface in the frequency range of 10^{-2}–10^6 Hz.

3. Results and discussion

Fig. 1 shows a typical SEM and AFM image of the precipitate obtained as described in the experimental section at different magnifications. Plate like nanoparticles with a polygonal edge of diameter ~250–300 nm are obvious from Fig. 1a–d. The atomic force microscopy (AFM) image (Fig. 1c–d, topography) demonstrates that the large quantity of homogeneous nanoplates formed during precipitation. Fig. 2a–c shows clearly the cross-section of a typical hexagonal nanoplates which is ~270×500 nm^2. Fig. 2a cross-sectional plot shows a dip of depth ~90 nm indicating the height of a nanoplate from its adjacent bottom layer. The diagonal length of a typical hexagonal nanoplates is determined by drawing a line along the diagonal (Fig. 2b). The vertical arrows (↓) in cross-

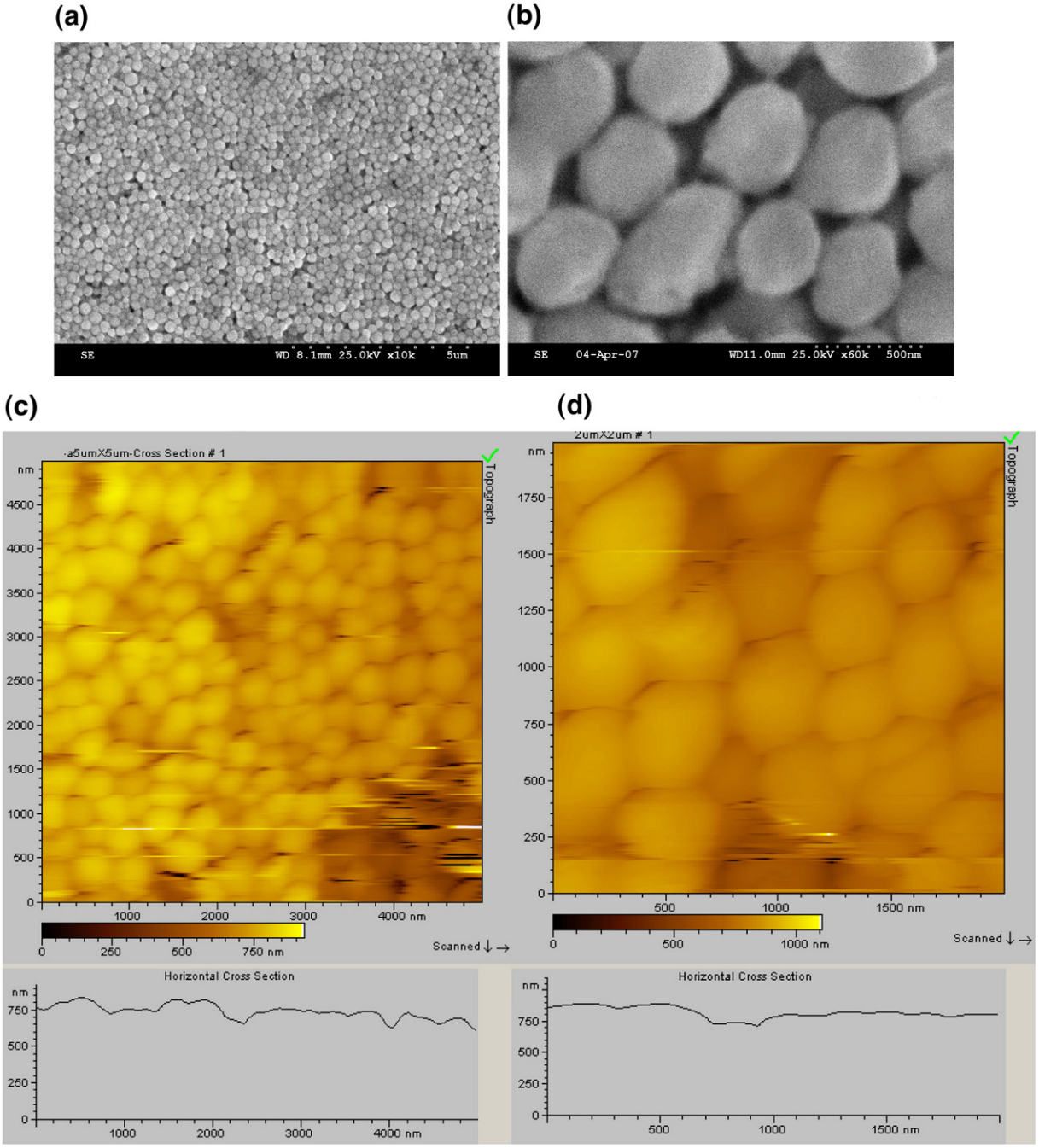

Fig. 1. SEM Micrograph of as-prepared AgCl nanoplates at different magnifications (a) 10 k (b) 60 k (scales are shown on the images). (c)–(d) morphologies of the as-prepared AgCl nanoplates through AFM topography obtained using capping agent PDADMAC as described in experimental section.

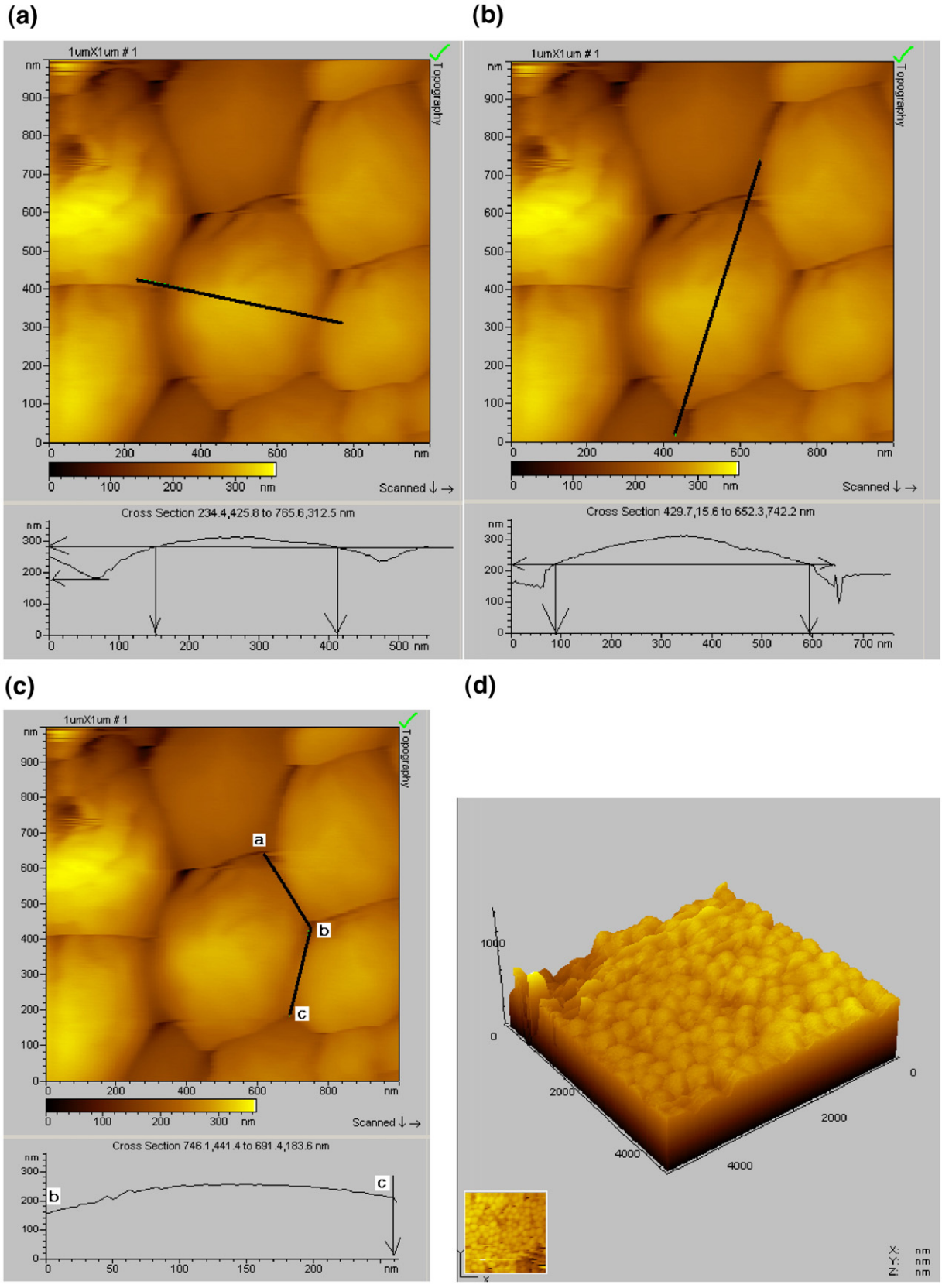

Fig. 2. Cross-sectional determination of nanoplates using AFM topographical images (a) a line is drawn along the width on the nanoplate. The vertical line (↓) in the cross-sectional plot indicates the width of a typical hexagonal nanoplates ~270 nm. However, the horizontal arrows (←) touching to *y*-axis indicates height of nanoplates from its adjacent bottom layer. (b) Shows diagonal length determination of a typical nanoplates. The vertical arrow (↓) in the cross-sectional plot indicates the diagonal length ~500 nm. (c) Edge length determination of a typical hexagonal nanoplates which is ~ab=bc~300 nm. (d) Three-dimensional view of the nanoplates deposited on substrates.

sectional plot of Fig. 2b shows the diagonal length of nanoplates is ~500 nm. Fig. 2a shows that the distance between vertical arrows is ~270 nm. So the cross-section of a typical hexagonal plate is ~270×500 nm^2. Again the AFM image (Fig. 2c, ab=bc~300 nm) confirm the edge diameter of nanoplates to be ~300 nm. Fig. 2d shows a three-dimensional view of the nanoplate film deposited on glass substrate by drop cast method. Moreover, the EDAX study of sample shows only the presence of silver and chlorine without any other element contamination.

Fig. 3a further shows the XRD pattern of the synthesized precipitates of high purity AgCl. All the diffraction peaks can be readily indexed to an FCC phase of silver chloride with the lattice constant $a=b=c=5.549$, $\alpha=\beta=\gamma=90°$ (JCPDS-00-006-0480 or JCPDS no.31-1238). The crystallite size is ~32 nm calculated from XRD pattern using Debye–Scherrer equation. The thermal stability of as-prepared samples studied by differential thermal analyzer (DSC) (Fig. 3b). A transition to a melting phase occurs for as-prepared AgCl as obvious from Fig. 3b. It is evident that enthalpy of melting of the as-prepared AgCl is higher in heating cycle (~83.61 J/g) than that in the cooling cycle (~70.42 J/g). These fusion enthalpies are lower in magnitude with respect to the pristine silver chloride (ΔH~91.08 J/g) [27–30]. This decrease

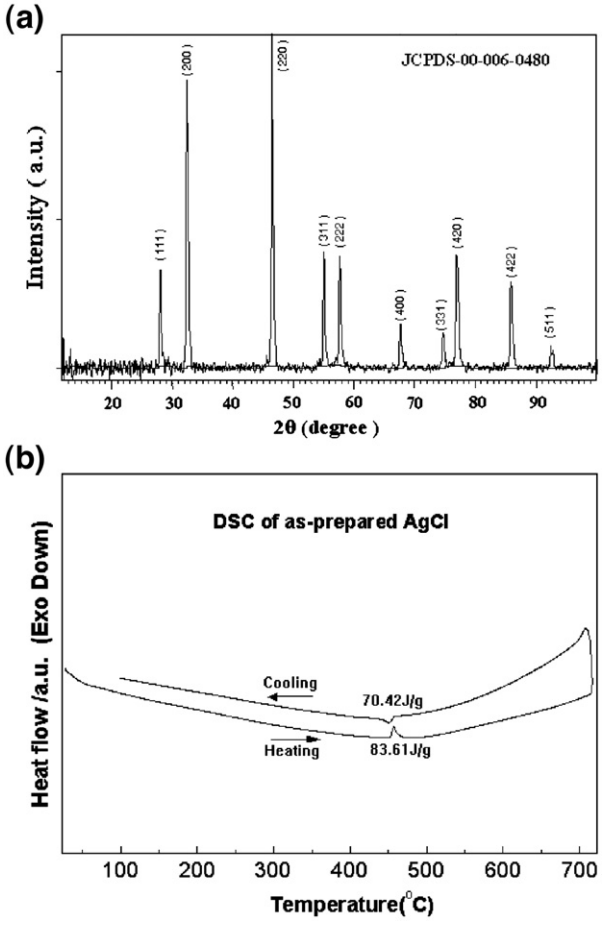

Fig. 3. (a) X-ray diffraction of as-prepared nanoplates showing corresponding JPCPDS file and *hkl* values of all the corresponding peaks. (b) DSC curve observed for the as-prepared AgCl nanoplates using Al_2O_3 as reference at the heating rate of 10 °C/min.

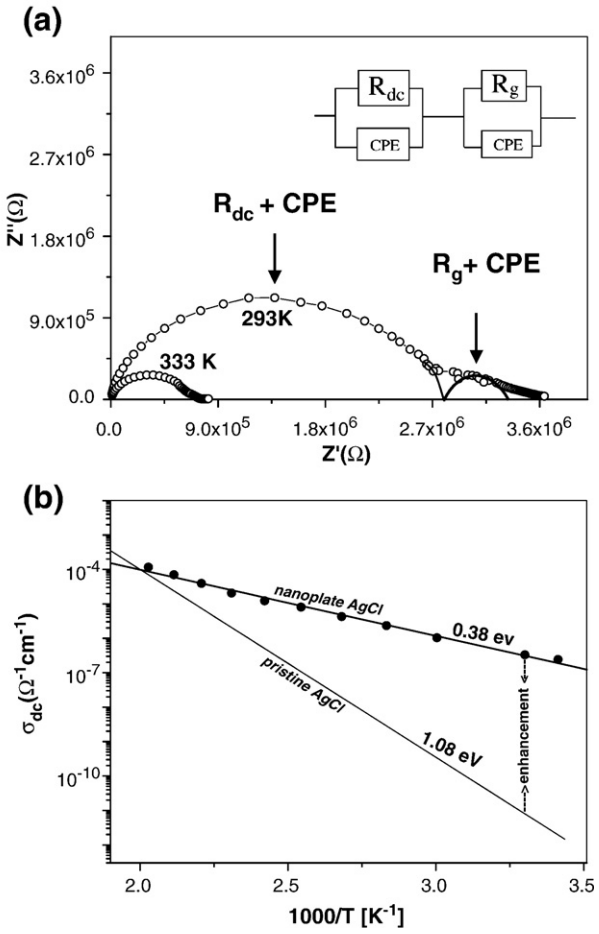

Fig. 4. (a) Impedance plot for the AgCl nanoplates at temperatures 293 K and 333 K. Inset: shows the equivalent circuit and it is clearly indicated by an arrow that constant phase element with bulk impedance (R_{dc}) represents a depressed semicircle in impedance plot with larger diameter and the grain boundary impedance (R_g) along with a constant phase element (CPE) represents the impedance plot as shown by a small circle with smaller diameter. The tail at lower frequencies in the impedance plot shows the effect of polarization at electrode–electrolyte interface. (b) Arrhenius plot of ionic conductivity of AgCl nanoplates and that of the pristine AgCl. The data shown in the plot for nanoplates of AgCl are our own data measured as described in experimental section. However, data shown for pristine AgCl is according to Refs. [26–29] (data of conductivity for pristine AgCl between 363 and 500 K are reproduced from Refs. [26–29] and plot below 363 K is extended Arrheniously) It is clear that nanoplates show higher conductivity with respect to the pristine AgCl.

of heat of fusion (melting) may be attributed to more disordered phase of the nanoplates. The heating cycle melting phase transition occurs at 456 °C, which is almost same for the cooling cycle phase transition temperature (~454 °C) at the heating rate of 10 °C/min.

Fig. 4a shows a typical impedance spectrum of the pressed nanoplates in the frequency range of 10^{-2}–10^6 Hz. At the ambient temperature (293 K), the impedance spectrum is a depressed semicircle accompanied by a small semicircle at the low frequency end. Such non-ideal semicircular plot may be due to presence of distributions of the relaxations times [31]. The equivalent circuit may consist of a bulk resistance (R_{dc}) in parallel with a constant phase element (CPE), connected in series with a grain boundary resistance (R_g) with again a constant phase element in parallel as shown in the inset of Fig. 4a. The incomplete

arc determined by the constant phase element (CPE) and resistance R_g (see equivalent circuit in the inset of Fig. 4a) corresponds to the lower frequency values of the complex impedance in the frequency range investigated [31–32]. The intercept of larger diameter semicircle at the real axis yields the dc resistance, which is used for the calculation of the dc conductivity of the materials and is equal to $\sim 2.41\times10^{-7}\ \Omega^{-1}\ cm^{-1}$ for these nanoplates at 293 K. This conductivity is ~4 orders of magnitude higher than that of the pristine silver chloride [27–30] (see Fig. 4b). This drastic increase in conductivity may be attributed to the small thickness and morphology of unstable stacking fault arrangements present in the entire nanocrystalline material [16]. Fig. 4b shows dc conductivity as a function of inverse of temperature for nanoplates of AgCl (solid circles) and that of the pristine microcrystalline silver chloride (black line). It is apparent that the data in Fig. 4b can be described by a simple Arrhenius equation [31]. Clearly the activation energy (0.32 eV) for nanoplates is lower than that of the pristine silver chloride (1.08 eV). The lower activation energy of AgCl nanoplates with respect to pristine AgCl is consistent with the recent report [16] for the nanoplates of silver iodide.

Fig. 5 shows the frequency dependence of the real part of the complex conductivity for as-prepared silver chloride at various temperatures. The conductivity spectrum is very similar to those observed for different types of disordered solids [31,33]. At low frequencies, random diffusion of ionic charge carriers via, activated hopping gives rise to frequency-independent dc conductivity. However; as frequency increases the ac conductivity shows dispersion. This behaviour of conductivity is quite common in disordered solids and commonly known as universal dynamic response (UDR) [34], in which Jonscher power law gives ac conductivity represented by Eq. (1).

$$\sigma'(\omega) = \sigma_{dc}(T) + A(T)\omega^n, n<1 \quad (1)$$

Where dc conductivity (σ_{dc}) and parameter A are frequency-independent, and have Arrhenius temperature dependance [31]. The values of n lie between 0 and 1.The numerical values of the

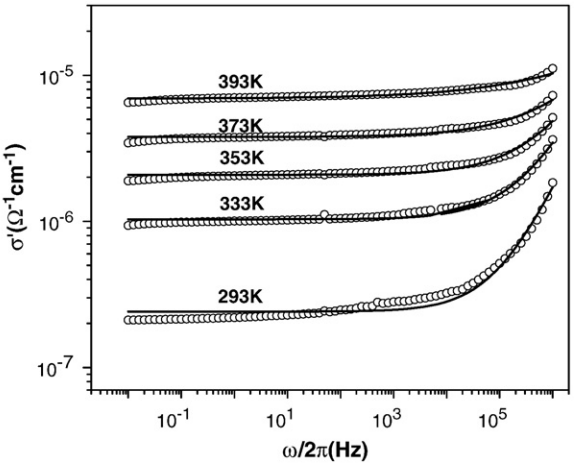

Fig. 5. The ac conductivity spectra for the silver chloride nanoplates at various temperatures. The solid line is the best-fit curve to the experimental data points according to universal dynamic response, viz., $\sigma'(\omega)=\sigma_{dc}(T)+A(T)\omega^n$, and $n<1$.

Table 1
Fitting parameters for the conductivity of the nanoparticles of AgCl spectra fitted in accordance with $\sigma'(\omega)=\sigma_{dc}(T)+A(T)\omega^n$

Temperature (K)	n	A (Ω^{-1} cm^{-1} s^n)	σ_{dc} (Ω^{-1} cm^{-1})
293	0.78	3.19×10^{-11}	2.41×10^{-7}
333	0.68	1.92×10^{-10}	1.03×10^{-6}
353	0.61	6.43×10^{-10}	2.08×10^{-6}
373	0.49	3.46×10^{-9}	3.78×10^{-6}
393	0.30	5.07×10^{-8}	6.93×10^{-6}

best-fit parameters of Eq. (1), $\sigma_{dc}(T)$, $A(T)$ and n at various temperature are listed in Table 1 with best-fit represented by solid line and data represented by open circle in the Fig. 5. However, a more detail investigations on the ion dynamics in these nanoplates are in progress and would be published soon.

4. Conclusions

In summary, we have successfully synthesized nanoplates of silver ion conductor (AgCl) at ambient temperature using the concept of capping agent (a surfactant). The synthesized nanoplates are found to be highly stable and have higher conductivity (~4 orders of magnitude) with respect to the microcrystalline silver ion conductor (AgCl). Mesoscopic effect may be a reason for the enhancement of conductivity of the material. The ac conductivity spectrum of this nanomaterial has similarities with that of the disorder solids and it can be well described by universal dynamic response (UDR).

Acknowledgements

Author acknowledges the Director (Prof. A. K. Shukla), Central Electrochemical Research Institute (CECRI) for his freedom for independent research, Professor A Kulkarni, Department of Metallurgical Engineering Indian Institute of Technology Mumbai (IIT-B, www.iitb.ac.in) for his help in electrical characterization and CSIR (India) for the short-term employment as a Quick Hire Fellow.

References

[1] B.C. Cheng, Z.G. Wang, Adv. Funct. Mater. 15 (2005) 1883.
[2] X.P. Gao, J.L. Bao, G.L. Pan, H.Y. Zhu, P.X. Huang, F. Wu, D.Y. Song, J. Phys. Chem., B. 108 (2004) 5547.
[3] Z.W. Pan, Z.R. Dai, Z.L. Wang, Science 291 (2001) 1947.
[4] S.J. Tans, M.H. Devoret, H.J. Dai, A. Thess, R.E. Smalley, L. Geerlings, J.C. Dekker, Nature 386 (1997) 474.
[5] R. Martel, T. Schmidt, H.R. Shea, T. Hertel, Ph. Avouris, Appl. Phys. Lett. 73 (1998) 2447.
[6] A.M. Morales, C.M. Lieber, Science 279 (1998) 208.
[7] X.F. Duan, Y. Huang, R. Agrawal, C. M Lieber, Nature 421 (2003) 241.
[8] J.F. Wang, M.S. Gudiksen, X. F Duan, Y. Cui, C.M. Lieber, Science 293 (2001) 1455.
[9] C.J. Mao, X.C. Wu, H.C. Pan, J.J. Zhu, H.Y. Chen, Nanotechnology 16 (2005) 2892.
[10] C. Li, D.H. Zhang, X.L. Liu, S. Han, T. Tang, J. Han, C.W. Zhou, Appl. Phys. Lett. 82 (2003) 2405.
[11] Y. Cui, Q.Q. Wei, H.K. Park, C.M. Lieber, Science 293 (2001) 1289.
[12] J. Kong, N.R. Franklin, C.W. Zhou, M.G. Chapline, S. Peng, K. Cho, H.J. Dai, Science 287 (2000) 622.

[13] D.H. Zhang, C. Li, S. Han, X.L. Liu, C.W. Zhou, Appl. Phys. A76 (2003) 163.
[14] H.L. Tuller, Solid State Ionics 131 (2000) 143.
[15] J. Maier, J. Electroceram. 13 (2004) 593.
[16] Yu-Guo Guo, Jong-Sook Lee, J. Maier, Adv. Mater 17 (2005) 2815.
[17] Yu-Guo Guo, Jong-Sook Lee, J. Maier, Solid State Ionics 177 (2006) 2467.
[18] M. Li, M. Shao, H. Ban, H. Wang, H. Gao, Solid State Ionics 178 (2007) 775.
[19] J. Schoonman, Solid State Ionics 157 (2003) 319.
[20] H.K. Liu, G.X. Wang, Z. Guo, J. Wang, K. Konstantinov, J. Nanosci. Nanotechnol. 6 (2006) 1.
[21] Yu-Guo Guo, Jong-Sook Lee, H.U. Yong-Sheng, J. Maier, J. Electrochem. Soc. 154 (2007) K51.
[22] X.G. Peng, L. Manna, W.D. Yang, J. Wickham, E. Scher, A. Kandavanich, A.P. Alivisatos, Nature 404 (2000) 59.
[23] S.-H. Yu, H. Colfen, K. Tauer, M. Antonietti, Nat. Matters 4 (2005) 51.
[24] J. Roged, O. Schaf, P. Knauth, Solid State Ionics 136–137 (2000) 955.
[25] A.P. Batra, L.M. Slifkin, Phys. Rev., B. 12 (1975) 3473.
[26] J. Corish, D.C. A Mulcahey, J. Phys. C. Solid State Phys. 13 (1980) 6459.
[27] S. Chandra, Superionic Solids: Principles and Applications, North Holland Publishing Company Amsterdam-New York-Oxford, 1981.
[28] N. Hainovsky, J. Maier, Phy. Rev., B. 51 (1995) 15789.
[29] J.K. Aboague, R.S. Friauf, Phys. Rev., B. 11 (1975) 1654.
[30] A.S. Skapin, J. Jamnik, S. Pejovnik, Solid State Ionics 133 (2000) 129.
[31] J.P. Tiwari, K. Shahi, Solid State Ionics 176 (2005) 1271.
[32] A.K. Shukla, V. Sharma, N.A. Dhas, K.C. Patil, Mater. Sci. Eng. B. 40 (1996) 153.
[33] K. Funke, Philos. Mag., A 68 (1993) 711.
[34] A.K. Jonscher, Nature 267 (1977) 673.